Electronic Supplementary Material (ESI) for Journal of Materials Chemistry A.
This journal is © The Royal Society of Chemistry 2018

3D reticulated carbon nitride materials high-uniformly capture 0D black phosphorus as 3D/0D composites for stable and efficient photocatalytic hydrogen evolution

Ting Song,[a] Gongchang Zeng,[b] Piyong Zhang,[a] Tingting Wang,[b] Atif Ali,[a] Shaobin Huang,[b] and Heping Zeng*,[a]

[a]Key Laboratory of Functional Molecular Engineering of Guangdong Province, School of Chemistry and Chemical Engineering, South China University of Technology, Guangzhou 510641, P. R. China.

[b]School of Environment and Energy, South China University of Technology, Guangzhou, 510006, P. R. China.

*****Corresponding author. Tel.: +86-20-87112631; Fax: +86-20-87112631; E-mail: hpzeng@scut.edu.cn;

The apparent Quantum Efficiency Measurement

The apparent quantum efficiency (AQE) was measured using the same experimental setup for the photocatalytic hydrogen evolution, but with an additional band-pass filter to obtain monochromatic light. Band-pass filters (420) were equipped when conducting reactions under photons of different wavelengths and collecting apparent quantum efficiency (AQE) results. The amount of H_2 produced in the first 5 h was used to calculate quantum efficiency using the equation below. The apparent quantum efficiency (AQE) was calculated by using the following equation:

$$\text{AQE} = \frac{2 \times \text{the number of evolved hydrogen molecules}}{\text{the number of incident photons}} \times 100\%$$

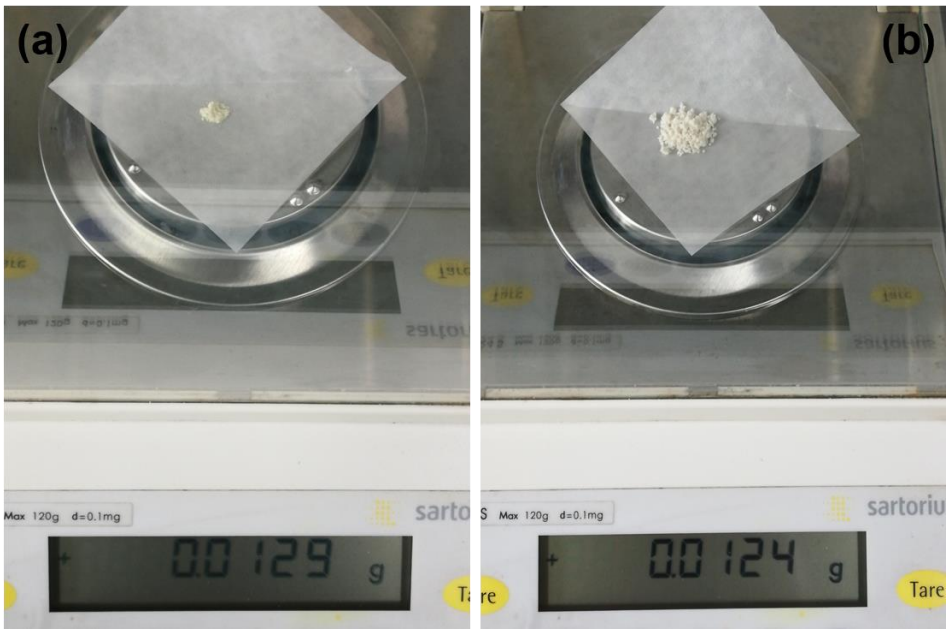

Fig. S1. Photographs of NCN and CN-4N.

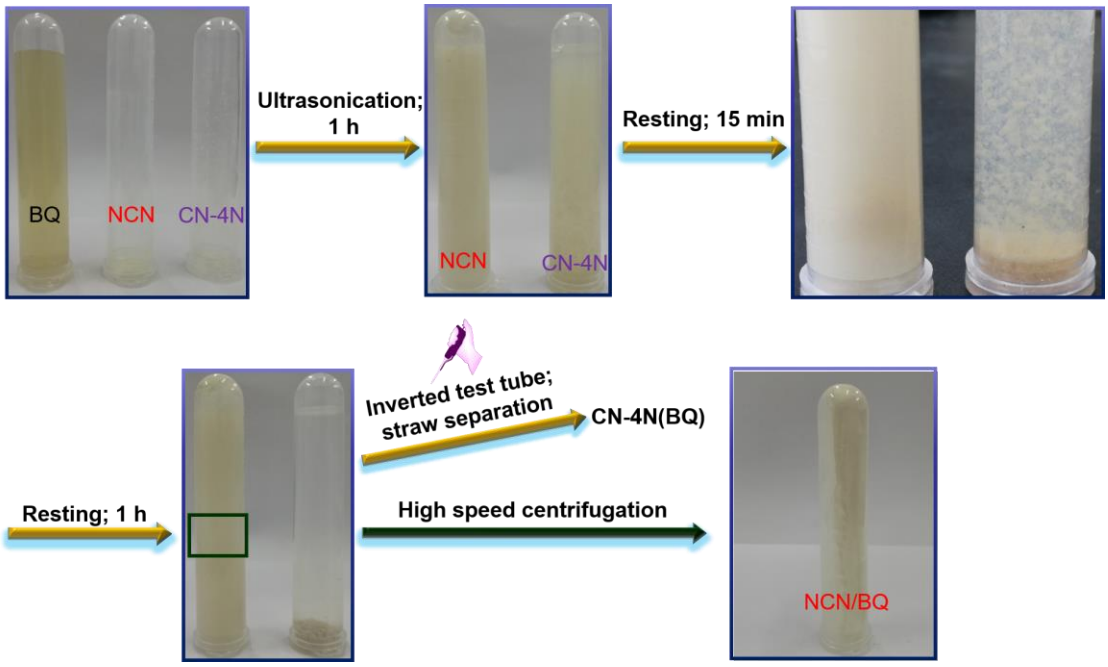

Fig. S2. Synthesis diagram of NCN/BQ and CN-4N(BQ) with self-capturing property.

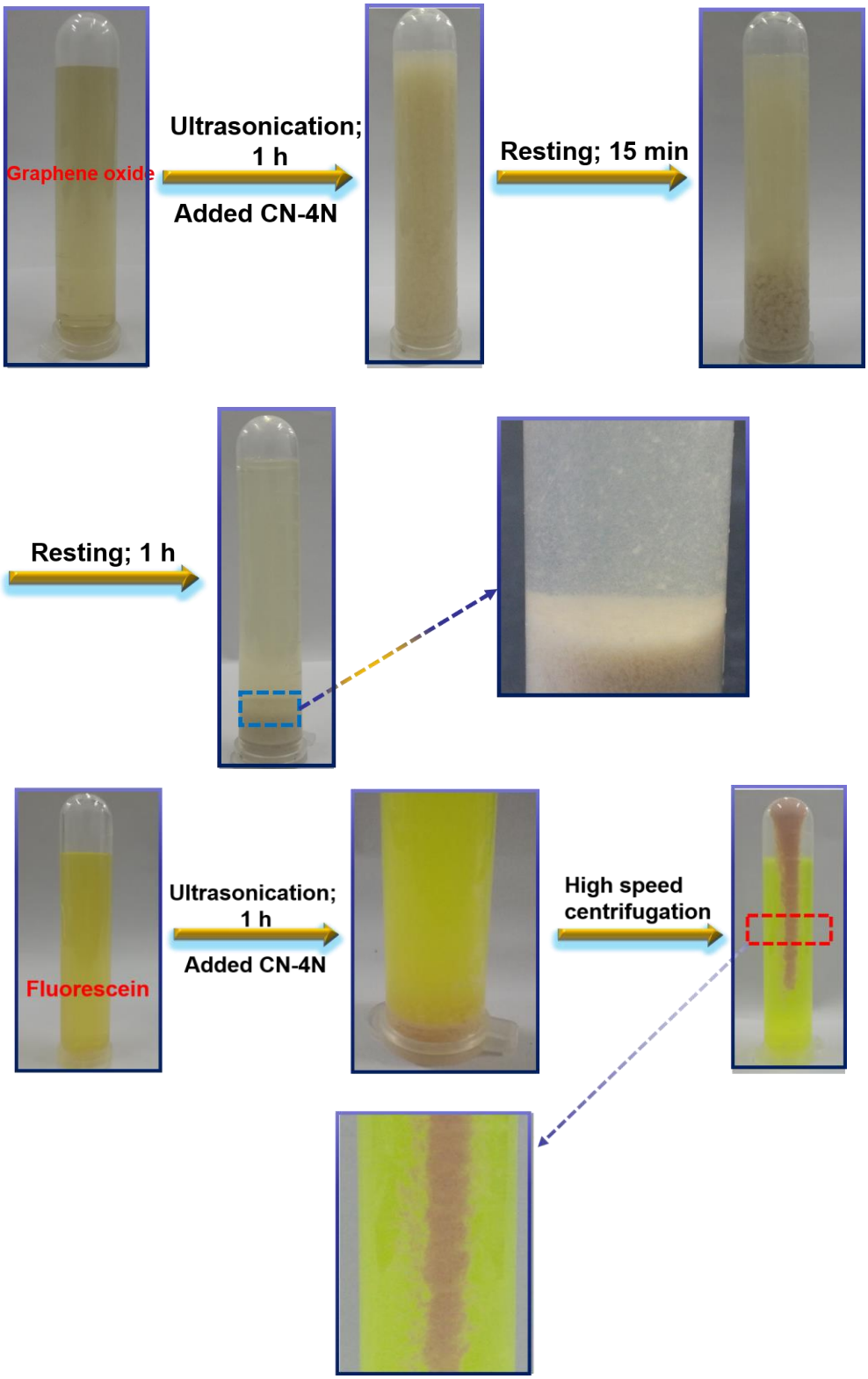

Fig. S3. Synthesis diagram of CN-4N(Graphene oxide) and CN-4N(Fluorescein) with self-capturing property.

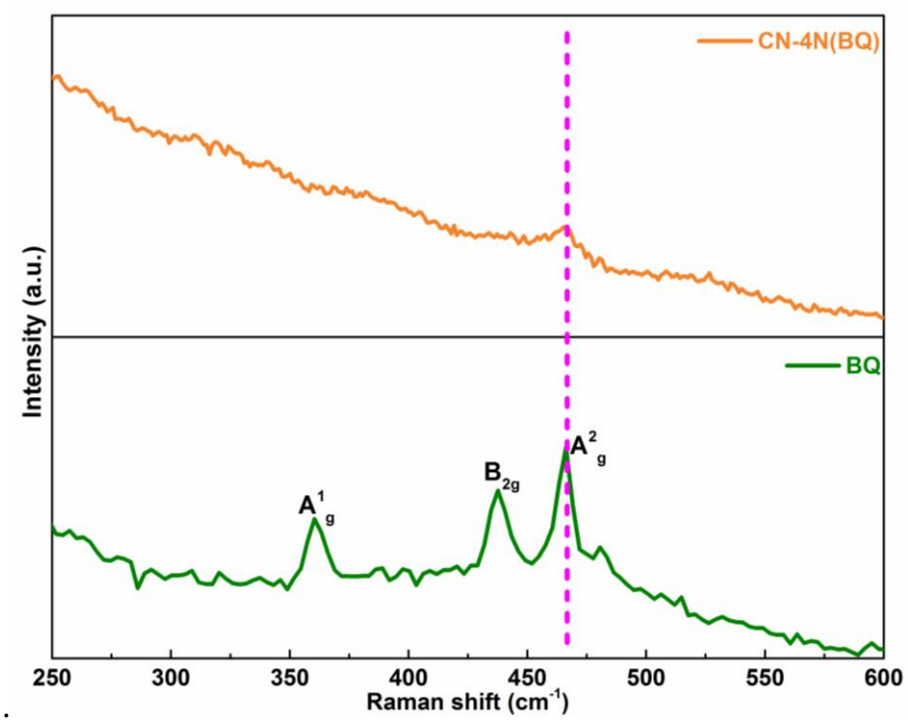

Fig. S4. Raman spectra of BQ and CN-4N(BQ).

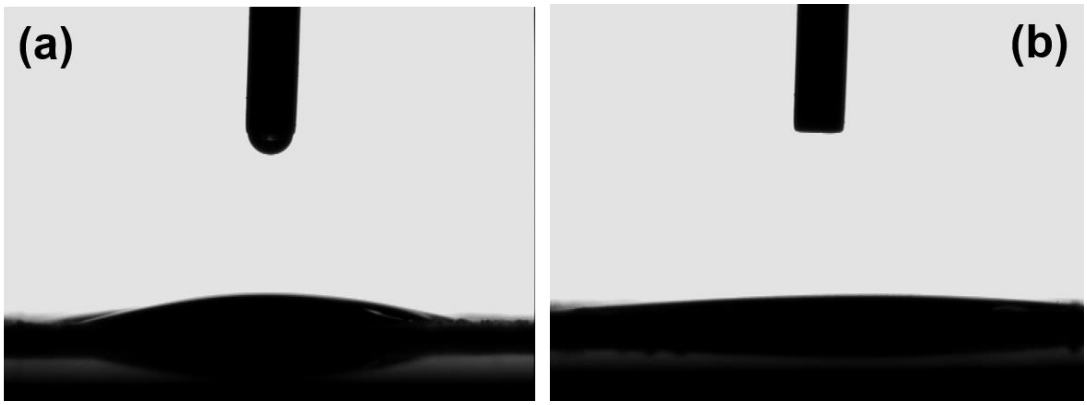

Fig. S5. The differences in hydrophilicity of NCN (a) and CN-4N (b) using contact angle measurements. Volume of the droplet is 5 μL.

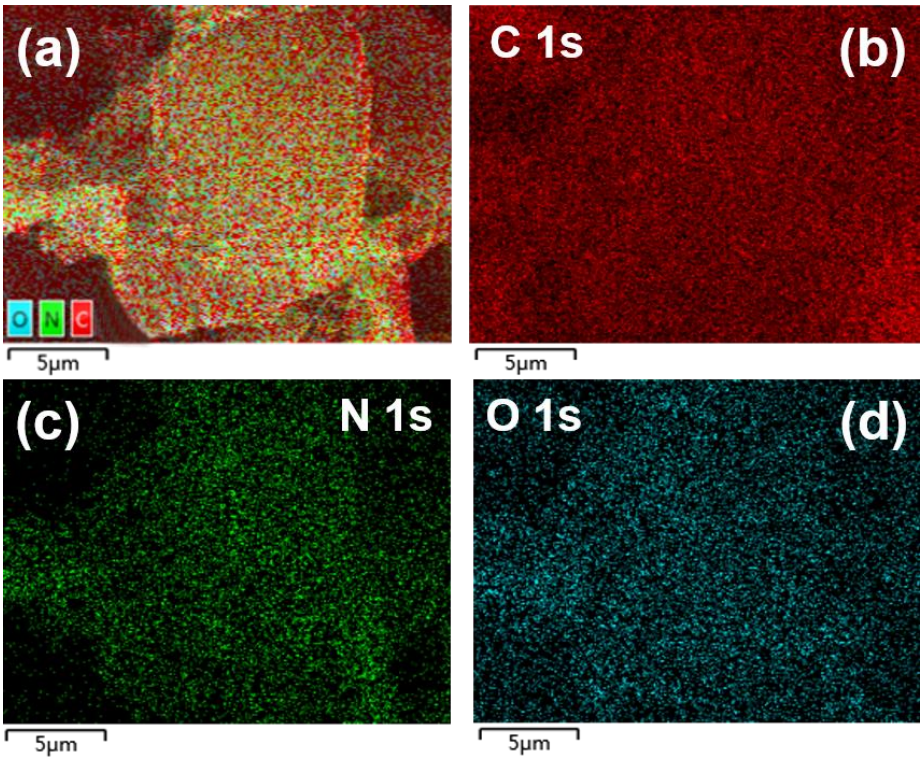

Fig. S6. Elemental mapping pattern of CN-air.

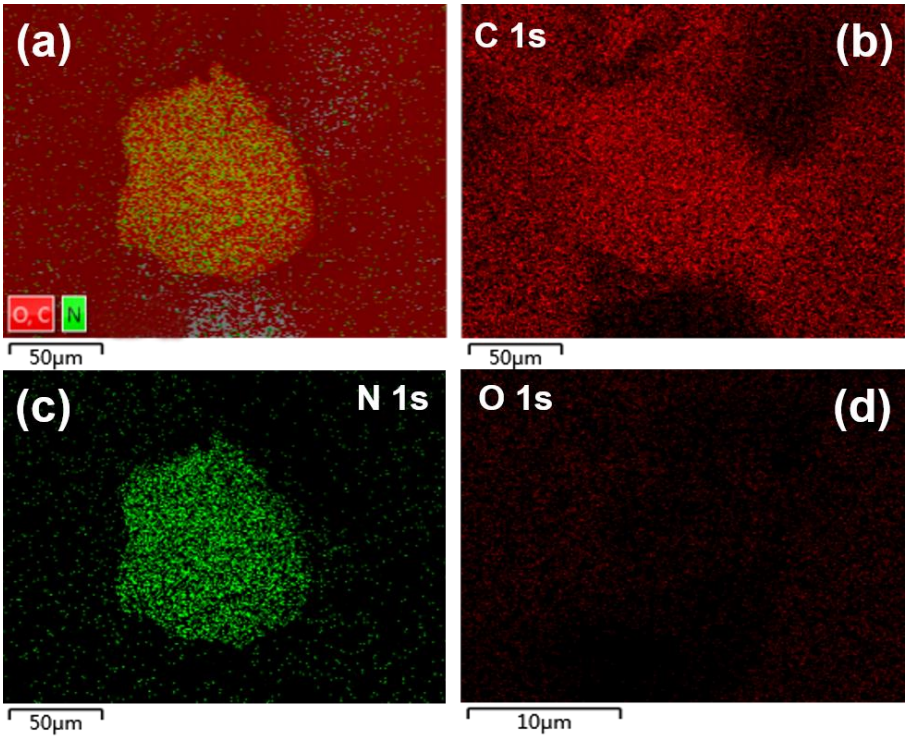

Fig. S7. The size distributions of pristine CN-4N.

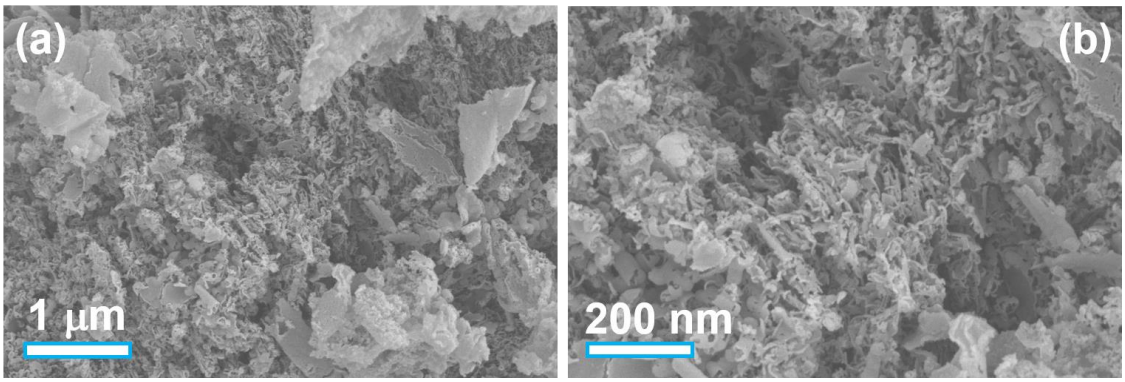

Fig. S8. SEM image of CN-4Ar.

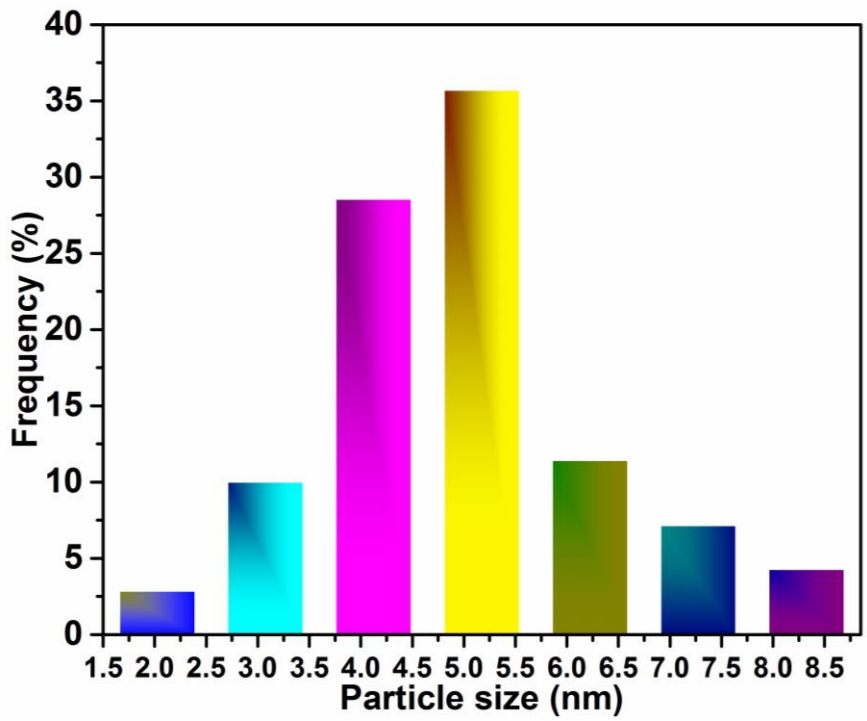

Fig. S9. The size distributions of pristine BQ.

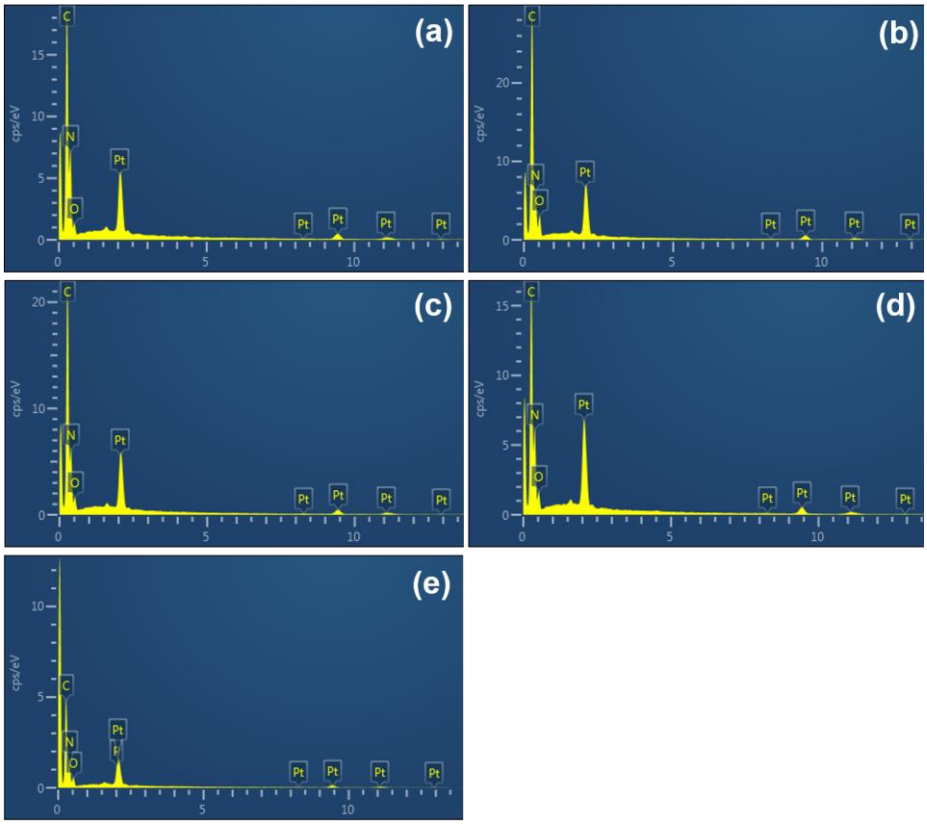

Fig. S10. EDS spectra of NCN, CN-air, CN-4Ar, CN-4N, and CN-4N(BQ), respectively.

Table S1 The C/N atomic ratio, oxygen atom, phosphorus atom, S_{BET}, and pore volume of as-obtained samples.

Sample	C/N atomic ratio	Oxygen atom (%)	Phosphorus atom (wt %)	S_{BET} (m^2/g)	Pore Volume
NCN	0.72	2.41	-	11.2	0.054
CN-4N	0.78	1.74	-	183.6	1.07
CN-4N(BQ)	0.75	2.84	1.16	178.1	1.13

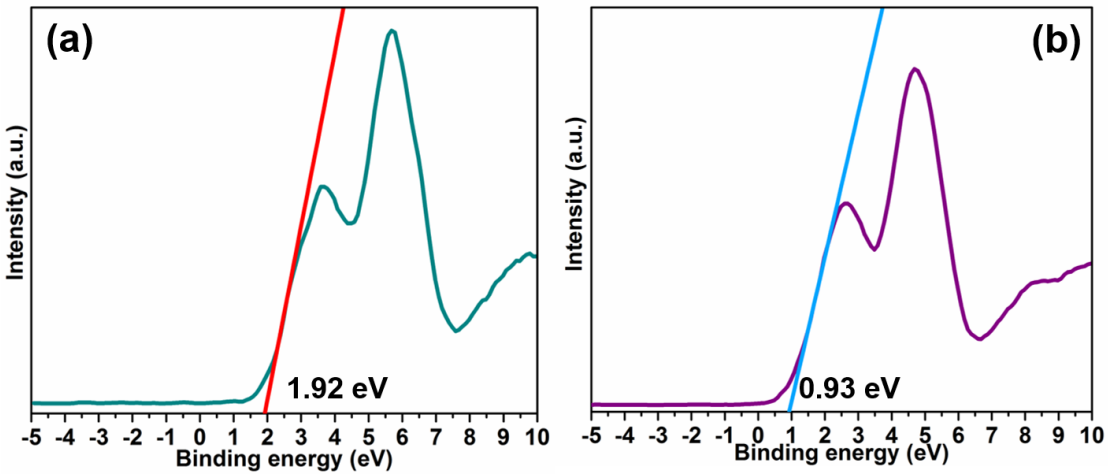

Fig. S11. The VB XPS of (a) CN-4N and (b) BQ.

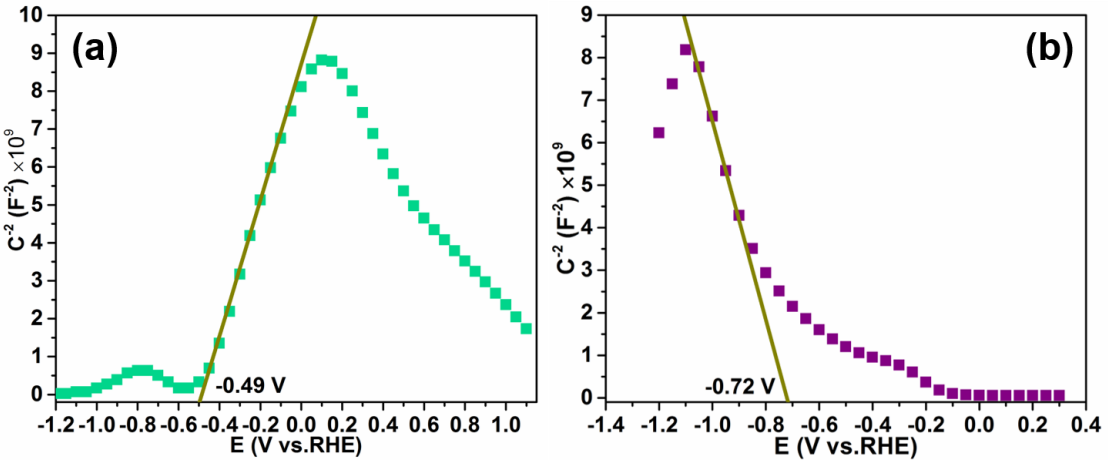

Fig. S12. Mott-Schottky plots for (a) CN-4N and (b) BQ electrodes.

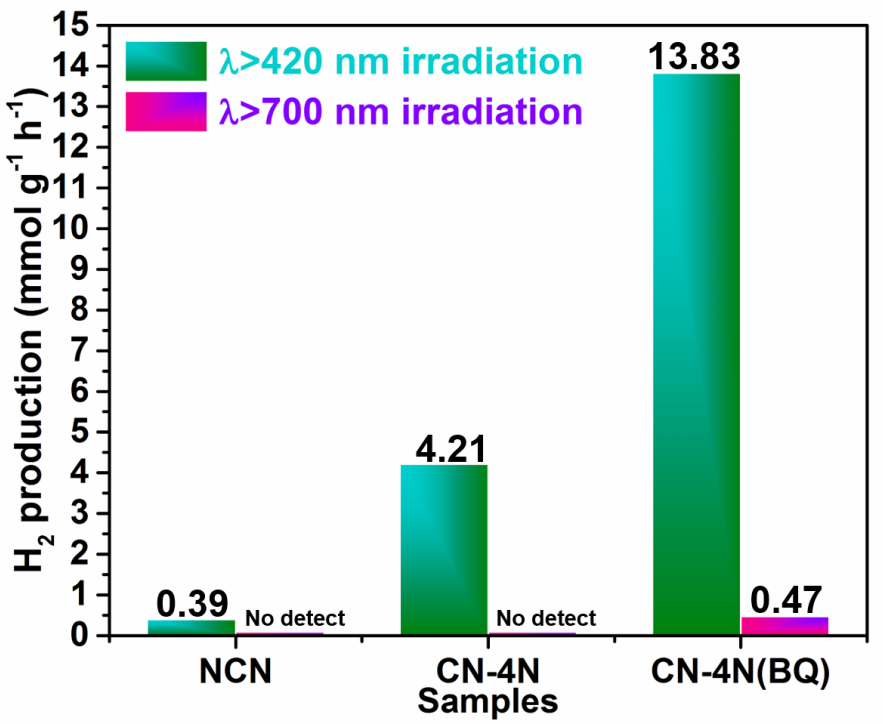

Fig. S13. Photocatalytic H_2 production from water on photocatalysts under λ> 420 nm and λ>700 nm irradiation.

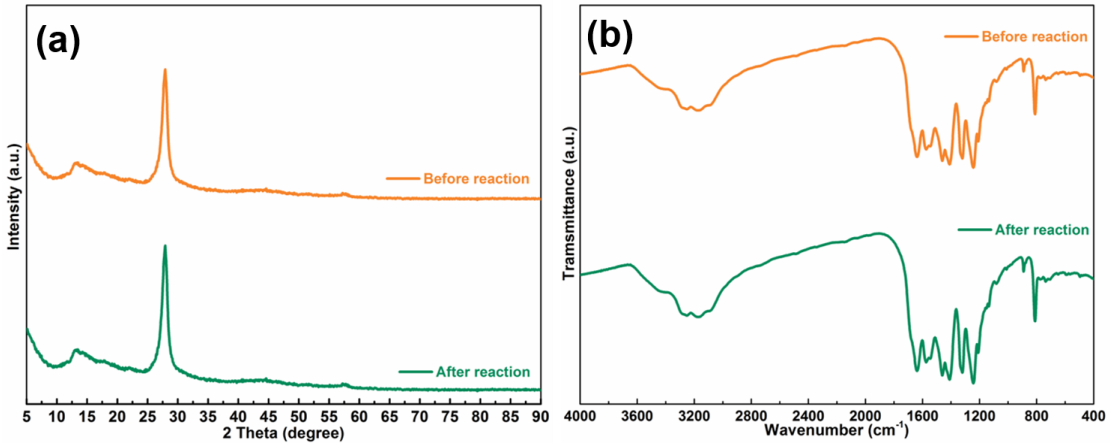

Fig. S14. XRD patterns (a) and FTIR spectra (b) of CN-4N(BQ) composite before and after the stability test.

Table S2 The comparation of photocatalytic H_2 production activity among some representative g-C_3N_4 photocatalysts reported in the literatures over recent years and ***this work***.

Photocatalyst	H_2 evolution rate ($\mu mol\ h^{-1}\ g^{-1}$)	Light source (nm)	Sacrificial agent (vol %)	Ehancement fators vs. bulk
CeO_2/g-C_3N_4 [S1]	73.12	300W Xe lamp λ≥ 420	20% lactic acid; 0.5 wt% Pt cocatalyst	1.5
Ni_2P@BP/g-C_3N_4 [S2]	852.2	300W Xe lamp λ≥ 420	10 vol% of TEOA	50
WO_3/g-C_3N_4 [S3]	12.3	250 W iron doped metal halide lamp λ≥ 420	No added	No offered
Nano-$InVO_4$/g-C_3N_4 [S4]	212	300W Xe lamp λ≥ 420	20% methanol; 0.5 wt% Pt cocatalyst	No offered
$CaIn_2S_4$/g-C_3N_4 [S5]	102	300W Xe lamp λ≥ 420	0.5 M Na_2S and 0.5 M Na_2SO_3 0.5 wt% Pt cocatalyst	3
BP/g-C_3N_4 [S6]	427	320W Xe lamp λ≥ 420	25% methanol	No offered
carbon-doped TiO_2/ g-C_3N_4 [S7]	5728	300W Xe lamp λ≥ 420	10 % TEOA 8% Pt cocatalyst	2.31
Ni_2P/g-C_3N_4 [S8]	474.7	300W Xe lamp λ≥ 420	10% TEOA	No offered
$Ca_2Nb_2TaO_{10}$/g-C_3N_4 [S9]	870.8	300W Xe lamp λ≥ 400	10% TEOA	2.8
Ta_2O_5/ g-C_3N_4 [S10]	36.4	300W Xe lamp λ≥ 420	20% methanol 0.5 wt% Pt cocatalyst	4.2
BQ/g-C_3N_4 [S11]	1900	200 W Xe lamp	10% methanol	3.45
Amorphous carbon/g-C_3N_4 [S12]	212.8	350W Xe lamp λ≥ 420	15% TEOA 1 wt% Pt cocatalyst	10
Organic carbon nanotubes/g-C_3N_4 [S13]	166.7	150W Xe lamp λ≥ 300	10% TEOA 1.5 wt% Pt cocatalyst	5
Ni_3N/g-C_3N_4 [S14]	169	300W Xe lamp λ≥ 420	10% TEOA	No offered
BQ/g-C_3N_4 [S15]	271	300W Xe lamp λ≥ 420	10% methanol	5.65
Ni_3C/g-C_3N_4 [S16]	303.6	350W Xe lamp λ≥ 420	17.6% TEOA	116.8
CQD/g-C_3N_4 nanotubes [S17]	3538.3	300W Xe lamp λ≥ 400	33.3% methanol 3 wt% Pt cocatalyst	2.5
Ni_2P/g-C_3N_4 [S18]	8400	300W Xe lamp λ≥ 400	10% TEOA	25.4
0D Black phosphorus /3D reticulated carbon Nitride **(This work)**	13830	300W λ≥ 420	10% TEOA 2 wt% Pt cocatalyst	35.4

References

[1] N. Tian, H. W. Huang, C. Y. Liu, F. Dong, T. R. Zhang, X. Du, S. X. Yu and Y. H. Zhang, *J. Mater. Chem. A*, 2015, **3**, 17120-17129.

[2] R. Boppella, W. Yang, J. W. Tan, H. C. Kwon, J. Park and J. Moon, *Appl. Catal. B: Environ*., 2019, **242**, 422-430.

[3] G. X. Zhao, X. B. Huang, F. Fina, G. Zhang and J. Irvine, *Catal. Sci. Technol*., 2015, **5**, 3416-3422.

[4] B. Hu, F. P. Cai, T. J. Chen, M. S. Fan, C. J. Song, X. Yan and W. D. Shi, *ACS Appl. Mater. Interfaces*, 2015, **7**, 18247-18256.

[5] D. L. Jiang, J. Li, C. S. Xing, Z. Y. Zhang, S. C. Meng and M. Chen, *ACS Appl. Mater. Interfaces*, 2015, **7**, 19234-19242.

[6] M. S. Zhu, S. Kim, L. Mao, M. Fujitsuka, J. Y. Zhang, X. C. Wang and T. Majima, *J. Am. Chem. Soc*., 2017, **139**, 13234-13242.

[7] C. W. Yang, J. Q. Qin, Z. Xue, M. Z. Ma, X. Y. Zhang and R. P. Liu, *Nano Energy*, 2017, 41, 1-9.

[8] D. Q. Zeng, W. J. Xu, W. J. Ong, J. Xu, H. Ren, Y. Z. Chena, H. F. Zheng and D. L. Peng, *Appl. Cataly. B: Environ.*, 2018, **221**, 47-55.

[9] S. Thaweesak, M. Lyu, P. Peerakiatkhajohn, T. Butburee, B. Luo, H. J. Chen and L. Z. Wang, *Appl. Catal. B: Environ.*, 2017, **202**, 184-190.

[10] Y. Z. Hong, Z. Y. Fang, B. X. Yin, B. F. Luo, Y. Zhao, W. D. Shi and C. S. Li, *Int. J. Hydrogen Energy*, 2017, **42**, 6738-6745.

[11] L. Q. Kong, Y. J. Ji, Z. Z. Dang, J. Q. Yan, P. Li, Y. Y. Li and S. Z. Liu, *Adv. Funct. Mater*., 2018, **28**, 1800668-1800678.

[12] Q. L. Xu, B. Cheng, J. G. Yu and G. Liu, *Carbon*, 2017, **118**, 241-249.

[13] K. C. Christoforidisa, Z. Syrgiannis, V. Parola, T. Montinia, C. Petitb, E. Stathatose, R. Godinf, J. Durrantf, M. Pratoa and P. Fornasiero, *Nano Energy*, 2018, **50**, 468-478.

[14] L. Chen, H. J. Huang, Y. H. Zheng, W. H. Sun, Y. Zhao, P. Francis and X. X. Wang, *Dalton Trans.*, 2018, **47**, 12188-12196.

[15] W. Y. Lei, Y. Mi, R. J. Feng, P. Liu, S. Hu, J. G. Yu, X. F. Liu, J. A. Rodriguez, J. O. Wang, L. Zheng, K. Tang, S. X. Zhu, G. Liu and M. H. Liu, *Nano Energy*, 2018, **50**, 552-561.

[16] K. L. He, J. Xie, Z. Q. Liu, N. Li, X. B. Chen, J. Hu and X. Li, *J. Mater. Chem. A*, 2018, **6** 13110-13122.

[17] Y. Wang, X. Q. Liu, J. Liu, B. Han, X. Q. Hu, F. Yang, Z. W. Xu, Y. C. Li, S. R. Jia, Z. Li and Y. L. Zhao, *Angew. Chem. Int. Ed*., 2018, **57**, 5765-5771.

[18] A. R. Indra, A. Acharjya, P. W. Menezes, C. Merschjann, D. Hollmann, M. Schwarze, M. Aktas, A. Friedrich, S. Lochbrunner, A. Thomas and M. Driess, *Angew. Chem. Int. Ed*., 2017, **56**, 1653-1657.